Performance Improvement of Large Sr^{2+} and Ba^{2+} co-doped $LaBr_3:Ce^{3+}$ Scintillation Crystals

Kan Yang, *Member, IEEE,* Peter R. Menge, *Member, IEEE,*
Jan J. Buzniak, and Vladimir Ouspenski

***Abstract*–The performance improvement of large size (ϕ = 60 mm, ℓ = 80 mm) Sr^{2+} and Br^{2+} co-doped $LaBr_3:Ce^{3+}$ scintillation crystals is reported. The scintillation light output of both Sr^{2+} and Br^{2+} co-doped crystals are significantly improved. Compared to 70,000 ph/MeV (at 662 keV) for Ce^{3+} only $LaBr_3$, Sr^{2+} and Ba^{2+} co-doping increase the light output by ~25% to 88,000 ph/MeV and 89,000 ph/MeV, respectively. The energy resolutions of both Sr^{2+} and Ba^{2+} co-doped crystals are improved over a wide energy range as well. The scintillation decay time is slightly lengthened with co-doping. No secondary slow component is observed. Co-doped crystals exhibit very similar emission and excitation characteristics to the Ce^{3+} only crystal. Both Sr^{2+} and Ba^{2+} show improved light output proportionality in the low energy range.**

I. Introduction

CERIUM doped lanthanum bromide ($LaBr_3:Ce^{3+}$) scintillation crystal possesses a unique combination of favorable scintillation characteristics [1], including high scintillation light output, excellent energy resolution, fast scintillation decay time, good density, and excellent energy proportionality. These make $LaBr_3:Ce^{3+}$ attractive for a variety of applications including geophysical radiation detection [2], medical imaging [3], homeland security [4] and radiation detection in space [5].

$LaBr_3$:5% Ce^{3+} has been successfully commercialized by Saint-Gobain Crystals and marketed under the trade name "BriLanCe® 380". Saint-Gobain Crystals has developed a reliable growth process which produces large diameter crack-free $LaBr_3$ crystals [6].

Altering the properties of scintillation materials by co-doping has been known to the research community for years. Ca^{2+} co-doping is shown to improve both scintillation light output and timing of $LSO:Ce^{3+}$ [7], as well as $LYSO:Ce^{3+}$ [8]. $LuAG:Pr^{3+}$ co-doped with Ga^{3+} is found to have reduced slow decay components due to suppressed anti-site defects [9]. $CeBr_3$ doped with aliovalent cations is shown to have increased fracture toughness [10]. Co-doping, as an effective method to optimize the performance of scintillation materials, is being intensively studied by Saint-Gobain Crystals. In this paper, we present the performance improvement of $LaBr_3:Ce^{3+}$ scintillation crystals recently achieved through Sr^{2+} and Ba^{2+} co-doping.

Manuscript received November 16, 2012.

Kan Yang is with Saint-Gobain Crystals, Hiram OH 44234 USA (telephone: 440-834-5697, e-mail: kan.yang@saint-gobain.com).

Peter R. Menge is with Saint-Gobain Crystals, Hiram OH 44234 USA (telephone: 440-834-5673, e-mail: peter.r.menge@saint-gobain.com).

Jan J. Buzniak are with Saint-Gobain Crystals, Hiram OH 44234 USA (telephone: 440-834-5621, e-mail: jan.j.buzniak@saint-gobain.com).

Vladimir Ouspenski is with Saint-Gobain Recherche, 39 Quai Lucien Lefranc 93303 Aubervilliers France (telephone +33 (0)1.48.39.65.98, e-mail: vladimir.vo.ouspenski@saint-gobain.com).

II. Experimental

All $LaBr_3$ crystals studied in this research were grown by Saint-Gobain Crystals. Crystals listed in Table 1 were wrapped with Teflon reflector and hermetically packaged in titanium housings with sapphire optical windows on one end. Each crystal was optically coupled to the sapphire window by a clear silicone rubber.

TABLE I. $LaBr_3$ Crystals Tested

Constituent	Dopant(s)*	Size and Shape
$LaBr_3$	5% Ce^{3+}	ϕ = 60 mm, ℓ = 80 mm, cylinder
$LaBr_3$	5% Ce^{3+} + 0.50% Sr^{2+}	ϕ = 60 mm, ℓ = 80 mm, cylinder
$LaBr_3$	5% Ce^{3+} + 0.17% Ba^{2+}	ϕ = 60 mm, ℓ = 80 mm, cylinder

*at % in the melt, with respect to La^{3+}

For absolute light output measurements, the packaged crystals were optically coupled to a Hamamatsu R1307 photomultiplier tube (PMT) with a modified voltage divider [6]. The integral quantum efficiency was calculated based on the wavelength-dependent quantum efficiency of R1307 PMT and the radioluminescence spectrum of each individual crystal. Low energy gamma rays were used (e.g. 662 keV) to prevent current saturation in the PMT.

For determination of light output proportionality, packaged crystals were optically coupled to an ET 9305 PMT with a modified voltage divider. Multiple sources including ^{22}Na, ^{57}Co, ^{60}Co, ^{129}I, ^{133}Ba, ^{137}Cs, ^{232}Th and ^{241}Am were used to characterize the scintillation light output and energy resolution at various γ-ray energies. At least 50,000 counts were collected for each peak of interest to ensure sufficient counting statistics.

UV Emission and excitation spectra were measured with a Varian Eclipse Spectrophotometer. UV light from a Xenon lamp selected by a monochromator was used to excite the crystals. Light emission from the same surface as excitation was then recorded by a PMT through the emission monochromator. Radioluminescence spectra were collected in the same spectrophotometer. A 10 mCi collimated ^{241}Am source (59.5 keV γ-rays) was mounted on the side of the packaged crystals and used as the excitation source. α's from

^{241}Am were shielded by the housing and not used to excite crystals.

For determination of scintillation time profiles, a Time Correlated Single Photon Counting (TCSPC) technique originated by Bollinger and Thomas was used [11]. Two Photonis XP20Y0 PMTs were used in start and stop channels. The stop PMT was located at approximately 50 cm from the sample crystal. An adjustable aperture was used to ensure that the stop PMT only detects single photon events. The stop-to-start count rate ratio was kept below 5% for all measurements. The system was calibrated by an ORTEC 462 time calibrator before the measurements.

III. Results and Discussions

A. Light Output and Energy Resolution

Table 2 compares the absolute light output of Ce^{3+} only, Sr^{2+} co-doped and Ba^{2+} co-doped $LaBr_3$:Ce^{3+} crystals. Both Sr^{2+} and Ba^{2+} co-doped crystals show significant improvement in scintillation light output (+25%) compared with Ce^{3+} only crystal, which is more than twice the light output of a traditional NaI:Tl^+ scintillation crystal [12]. Fig. 1 compares the energy spectra of a ^{232}Th γ-ray source.

Improvement in energy resolution is shown in Fig 2. Both Sr^{2+} and Ba^{2+} co-doping significantly improve the energy resolution of $LaBr_3$:Ce^{3+} crystals over a wide energy range. Table 3 compares the energy resolutions for the packaged crystals (ϕ = 60 mm, ℓ = 80 mm) at three representative γ-ray energies.

Although both the light output of Sr^{2+} and Ba^{2+} co-doped crystals increased about the same amount, compared with Ce^{3+} only crystals, Sr^{2+} appeared to have better impact on the energy resolution. One possible explanation is that Sr^{2+} co-doped crystal may have better uniformity than Ba^{2+} co-doped one. It is also possible that Sr^{2+} co-doped crystal has better light output proportionality than Ba^{2+} co-doped crystals, especially in the low energy range (below 100 keV).

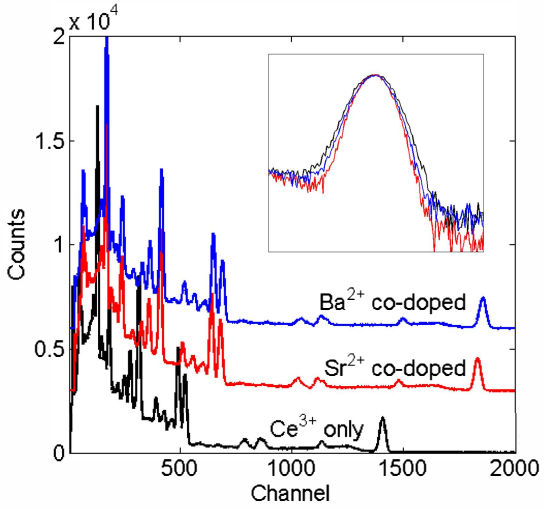

Fig. 1. ^{232}Th pulse height spectra of Ce^{3+} only, Sr^{2+} co-doped and Ba^{2+} co-doped $LaBr_3$:Ce^{3+} crystals; the insert compares the normalized 2.615 MeV energy peak measured three crystals.

TABLE II. Absolute Light Output[1,2]

Crystal	Absolute Light Output (ph/MeV)
Ce^{3+} only	70,000
Sr^{2+} co-doped	88,000
Ba^{2+} co-doped	89,000

[1] Measured on packaged crystals (ϕ = 60 mm, ℓ = 80 mm)
[2] Measured at 662 keV

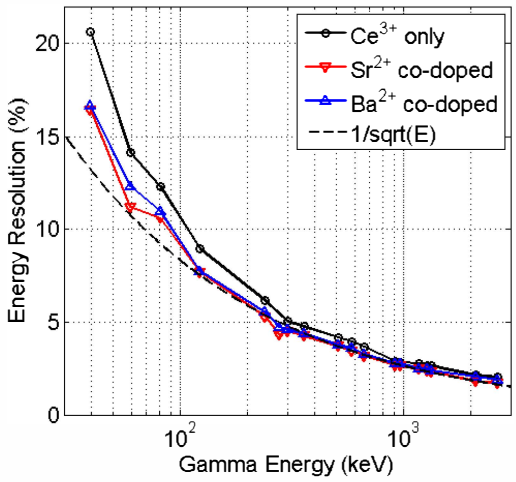

Fig. 2. Energy resolution as function of γ-ray energy deposition

TABLE III. Energy Resolution at Representative Energies*

Crystal	γ-ray Energies		
	122 keV	662 keV	2.615 MeV
Ce^{3+} only	9.0%	3.7%	2.0%
Sr^{2+} co-doped	7.7%	3.2%	1.7%
Ba^{2+} co-doped	7.7%	3.3%	1.9%

*Measured on packaged crystals (ϕ = 60 mm, ℓ = 80 mm)

B. Emission Characteristics

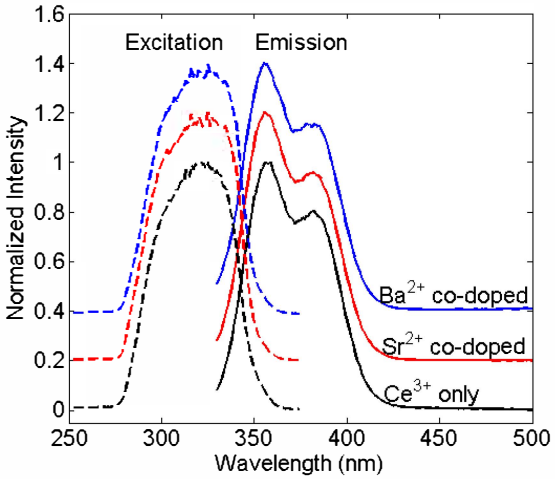

Fig. 3. UV emission and excitation spectra of Ce^{3+} only, Sr^{2+} co-doped and Ba^{2+} co-doped $LaBr_3$:Ce^{3+} crystals; excitation spectra were measured at 384 nm emission and emission spectra were measured under 320 nm UV excitation.

Fig. 3 shows UV excited emission and excitation spectra of Ce^{3+} only, Sr^{2+} co-doped and Ba^{2+} co-doped $LaBr_3$:Ce^{3+} crystals. All three crystals show characteristic double-peaked

emission from Ce^{3+} 5d to 4f ($^2F_{7/2}$, $^2F_{5/2}$) transitions, which is due to the split of Ce 4f level from spin-orbit coupling. The emission peaks for all three samples are at 356 nm and 382 nm. No resolvable peak shift is observed. The only difference is the intensity ratio of the 356 nm peak to 382 nm peak ($I_{356\ nm\ peak}/I_{382nm\ peak}$) for Ce^{3+} only crystal is slightly smaller than those for both Sr^{2+} and Ba^{2+} crystals. No additional emission peaks are observed in either Sr^{2+} or Ba^{2+} co-doped crystals.

Excitation spectra are very similar among samples, too. All of them show an excitation band from around 280 ~ 350 nm, peaked at ~325 nm. No significant difference can be resolved.

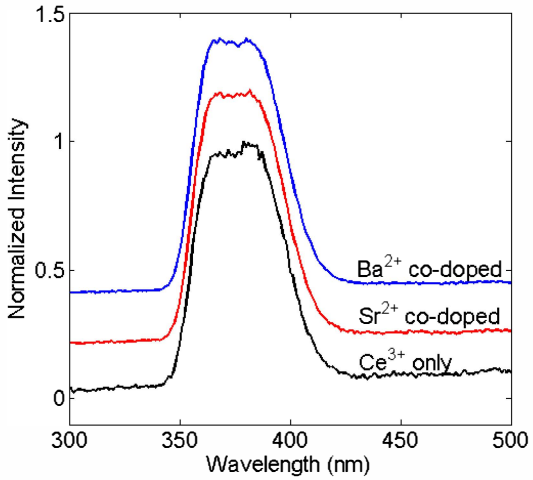

Fig. 4. Radioluminescence spectra of Ce^{3+} only, Sr^{2+} co-doped and Ba^{2+} co-doped $LaBr_3:Ce^{3+}$ crystals; spectra were measured under the excitation of 59.5 keV γ-ray from a 10 mCi ^{241}Am source.

Fig. 4 illustrates the γ-ray exited luminescence spectra of Ce^{3+} only, Sr^{2+} co-doped and Ba^{2+} co-doped $LaBr_3:Ce^{3+}$ crystals. The doublet structure is not well resolved. The two Ce^{3+} emission peaks are located at approximately 366 nm and 382 nm. All spectra are nearly identical except the intensity ratio of the 366 nm peak to 382 nm peak for Ce^{3+} only crystal is slightly smaller than those for both Sr^{2+} and Ba^{2+} crystals, which resembles the differences observed in UV excited emission.

Since the ^{241}Am source was mounted on the side of each crystal and the majority of the 59.5 keV γ-rays will be stopped in the first millimeter, the path length for γ-ray excited scintillation light to exit the crystal will be longer than that excited by UV, especially for these large crystals. For UV excited spectra, we measure the emission from the same surface which is excited by light. So the chance for scintillation light being absorbed and re-emitted by Ce^{3+} ions is higher for radioluminescence. The small red shift in the radioluminescence spectra indicates a certain level of Ce^{3+} self-absorption, which is also evidenced by the overlap between the excitation and emission spectra (Fig. 3).

C. Scintillation Time Profile

The scintillation time profiles of Ce^{3+} only, Sr^{2+} co-doped and Ba^{2+} co-doped $LaBr_3:Ce^{3+}$ crystals are shown in Fig. 5. All crystals have very similar decay time. Both Sr^{2+} and Ba^{2+} co-doping slightly lengthen the decay time of $LaBr_3:Ce^{3+}$ (Table 4). No additional secondary decay components are observed.

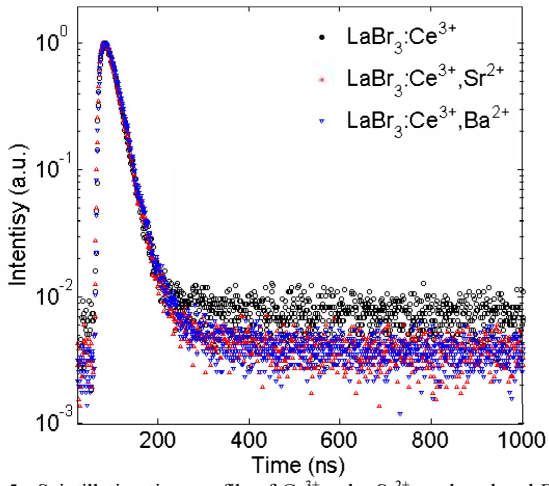

Fig. 5. Scintillation time profile of Ce^{3+} only, Sr^{2+} co-doped and Ba^{2+} co-doped $LaBr_3:Ce^{3+}$ crystals

TABLE IV MEASURED AND DECONVOLVED SCINTILLATION DECAY TIMES

Crystal	Measured Decay Time (ns)*	Deconvolved Decay Time (ns)
Ce^{3+} only	22.3	17.2
Sr^{2+} co-doped	24.8	18.2
Ba^{2+} co-doped	25.6	19.1

*Measured on packaged crystals (ϕ = 60 mm, ℓ = 80 mm)

Typical values for the decay time of the $LaBr_3:Ce^{3+}$ scintillation pulses are 16 ± 2 ns [13]. Note that the decay times measured by the Bollinger-Thomas method shown in Fig. 5 are several nanoseconds longer. The lengthening is due to the relative large size of the crystals, compounded by the high index of refraction of ~2.3 at 380 nm [14]. For large crystals, there is a greater absolute variation in the path length of the individual photons. This is illustrated in Fig. 6. The solid curve in Fig. 6 shows the impulse response function for light generated within the $LaBr_3$ crystal packages as calculated from simulation [15]. This curve is a histogram of photon arrival times at the PMT. Ten thousand scintillation pulses were generated randomly throughout the crystal volume. All the photons are generated at the same instant, and thus, the distribution in time is only due to the variation in path lengths of the photons. The pulses shown in Fig. 5 can be deconvolved using this impulse response function. An example deconvolution of the Sr^{2+} co-doped crystal pulse is the dashed curve in Fig. 6. The decay time of this deconvolved pulse is 18.2 ns. Table 4 compares the decay times of the deconvolved pulses. A slight difference exists among the 3 crystals, and the co-doped crystals show slightly longer decay times. Whether this is a real effect or simply experimental variation is still an open question. A future experiment will measure the pulse shape of small crystals.

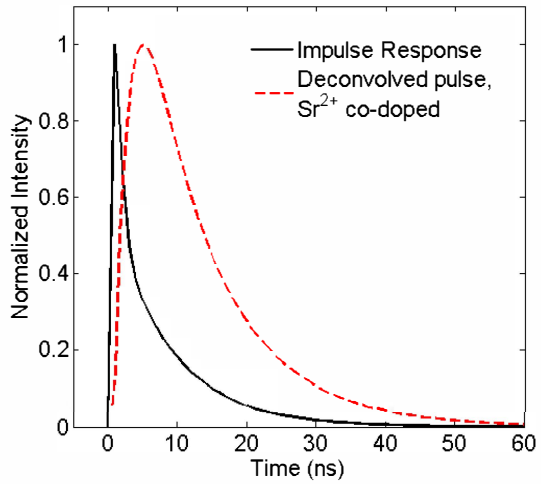

Fig. 6. Graph of the impulse response function for a $LaBr_3$ crystal (ϕ = 60 mm, ℓ = 80 mm), solid curve. The dashed curve is the deconvolution of the measured pulse from Fig. 5. The deconvolved decay time is 18.2 ns.

D. Proportionality

Fig. 7 compares the relative unit light output between Ce^{3+} only and co-doped crystals. The light output proportionality of Sr^{2+} and Ba^{2+} co-doped crystals are very similar over a wide energy range and are both better than the proportionality of Ce^{3+} only crystal. Improvement in light output proportionality, along with increased light output, contributes to the significant improvement in energy resolution for Sr^{2+} and Ba^{2+} co-doped crystals.

We are constructing a Compton coincidence experiment to better characterize the proportionality of co-doped crystals [16]. Results will be published in future reports.

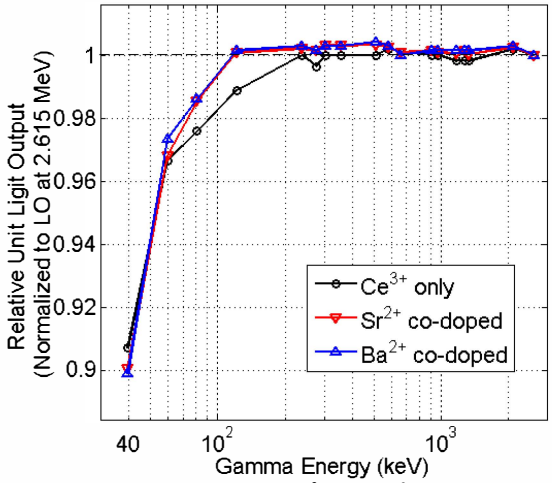

Fig. 7. Relative unit light output of Ce^{3+} only, Sr^{2+} co-doped and Ba^{2+} co-doped $LaBr_3:Ce^{3+}$ crystals as a function of deposited γ–ray energy; the relative unit light outputs are normalized to the unit light out of the same crystal at 2.615 MeV.

IV. Summary

Co-doping $LaBr_3:Ce^{3+}$ scintillation crystal with Sr^{2+} or Ba^{2+} improves its scintillation light output, energy resolution, and proportionality with no significant change in emission characteristics. Although the scintillation decay time was slightly lengthened by Sr^{2+} and Ba^{2+} co-doping, no secondary slow decay components were observed.

While it is clear that co-doping with Sr^{2+} and Ba^{2+} can be used to significantly improve the scintillation properties of $LaBr_3:Ce^{3+}$, the mechanism that how the aliovalent co-dopants improve the crystal remains unclear. Even though large size crystals are generally used in real applications, emission and timing characteristics could be altered due to various size-related effects including self-absorption and dispersion of photon path. Occasionally this can be beneficial, since a greater proportion of the scintillation light is shifted longer in wavelength where many photosensors are more sensitive. In order to further investigate the scintillation mechanism, small crystals will be prepared and studied. In addition, how Sr^{2+} co-doped and Ba^{2+} co-doped $LaBr_3:Ce^{3+}$ perform at high temperature is also an interesting subject. More results will be available in future reports.

Acknowledgment

The authors would like to thank Brian Bacon for his excellent work on crystal packaging.

References

[1] E.V.D. van Loef, P. Dorenbos, C.W.E. van Eijk, K. Krämer, and H.U. Güdel, *Applied Physics Letters*, vol. 79, pp. 1573-1575, 2001.

[2] C. Stoller, B. Adolph, M. Berheide, T. Brill, P. Clevinger, S. Crary, B. Crowder, S. Fricke, J. Grau, M. Hackbart, S. Herron, B. Jorion, M. Lorente, D. Madio, J. Miles, O. Philip, R.J. Radtke, B. Roscoe, I. Shestakova, W. Ziegler, P.R. Menge, *2011 Nuclear Science Symposium and Medical Imaging Conference,* vol., no., pp.191-195, 23-29 Oct. 2011.

[3] M. E. Daube-Witherspoon, S. Surti, A. Perkins, C. C. M Kyba, R. Wiener, M. E. Werner, R. Kulp and J. S. Karp, *Phys. Med. Biol.* vol.55 pp. 45, 2010.

[4] B.D. Milbrath, B.J. Choate, J.E. Fast, W.K. Hensley, R.T. Kouzes, J.E. Schweppe, *Nucl. Instrum. Methods. Phys. Res. A*, vol. 572, no. 2, pp. 774-784, Mar 2007.

[5] A. Owens, *IEEE Trans. Nucl. Sci.*, vol.55, no.3, pp.1430-1436, June 2008.

[6] P. R. Menge, G. Gautier, A. Iltis, C. Rozsa, and V. Solovyev, Nucl. Instrum. Meth. A, vol. 579, pp. 6-10, 2007.

[7] M. A. Spurrier, P. Szupryczynski, K. Yang, A. A. Carey, and C. L. Melcher, *IEEE Trans. Nucl. Sci.*, vol. 55, no. 3, pp. 1178–1182, 2008.

[8] S. Blahuta, B. Viana, A. Bessiere, V. Ouspenski, presented at *Nuclear Science Symposium and Medical Imaging Conference,* N26-6, 2012.

[9] M. Nikl,J. Pejchal, E. Mihokova, J. A. Mares, H. Ogino, A. Yoshikawa, T. Fukuda, A. Vedda, and C. D'Ambrosio, *Applied Physics Letters* vol.88, pp. 141916, 2006.

[10] M. J. Harrison, P. Ugorowski, C. Linnick, S. Brinton, D. S. McGregor, F. P. Doty, S. Kirpatrcik, and D. F. Bahr, *Proc. SPIE 7806, Penetrating Radiation Systems and Applications XI,* 78060M, Sept. 2010.

[11] L. M. Bollinger, G. E. Thomas, *Review of Scientific Instruments*, vol.32, no.9, pp.1044-1050, 1961.

[12] G.F. Knoll, *Radiation Detection and Measurement, 4th edition,* ISBN: 978-0-470-13148-0, pp. 238, John Wiley & Sons, Inc., 2010.

[13] G. Bizarri and P. Dorenbos, *Phys. Rev. B*, vol. 75, no. 184302, 2007.

[14] H.T. van Dam, S. Seifert, W. Drozdowki, P. Dorenbos and D.R. Schaart, *IEEE Trans. Nuc. Sci.*, vol. 59 (3), pp. 656, 2012.

[15] G.F. Knoll, T.F. Knoll and T.M. Henderson, *IEEE Trans. Nuc. Sci.*, vol. 35, pp. 872, 1988.

[16] P.B. Ugorowski, M.J. Harrison, D.S. McGregor, *Nucl. Instrum. Methods. Phys. Res. A*, 615, 2, pp.182-187, 2010.